FEBS Letters 585 (2011) 128–132

FEBS Letters

journal homepage: www.FEBSLetters.org

Enhanced acetylation of alpha-tubulin in influenza A virus infected epithelial cells

Matloob Husain *, Kevin S. Harrod

Infectious Diseases Program, Lovelace Respiratory Research Institute, Albuquerque, NM 87108, USA

ARTICLE INFO

Article history:
Received 1 October 2010
Revised 27 October 2010
Accepted 12 November 2010
Available online 19 November 2010

Edited by Jacomine Krijnse-Locker

Keywords:
Influenza A
Tubulin
Acetylation
Histone deacetylase 6
Rho

ABSTRACT

Acetylated microtubules (AcMTs), a post-translationally modified form of microtubules, promote polarized protein transport. Here we report that influenza A virus (IAV) induces the acetylation of microtubules in epithelial cells. By employing specific inhibitors and siRNA we demonstrate Rho GTPase-mediated downregulation of tubulin deacetylase activity in IAV-infected cells, resulting in increased tubulin acetylation. Further, we demonstrate that depolymerization/deacetylation or enhanced acetylation of microtubules decreased or increased, respectively, the release of virions from infected cells. IAV assembly requires the polarized delivery of viral components to apical plasma membrane. Our findings suggest the potential involvement of AcMTs in polarized trafficking of IAV components.

1. Introduction

Cytoskeleton is actively involved in virus entry, assembly, and release [1,2]. Cytoskeleton has been proposed to be involved in influenza A virus (IAV) assembly too [3]; however, a precise role of cytoskeletal elements is not understood. IAV causes an acute febrile respiratory disease in humans. IAV, an enveloped virus, is the prototype of family Orthomyxoviridae and possesses a segmented negative-sense RNA genome [4]. It replicates in the nucleus, assembles at the plasma membrane and is released by budding [5]. IAV assembly requires the polarized delivery of viral components to apical plasma membrane. IAV particle consist of three major components: the viral envelope, matrix protein (M1), and viral ribonucleoprotein (vRNP) core. During assembly, constituents of viral envelope are directly transported to the plasma membrane via exocytic pathway. However, transport mechanism of M1 and vRNP to the plasma membrane is not fully understood. The likely possibilities are that they use a piggy-back mechanism on viral transmembrane proteins or cytoskeletal elements [3]. Previously, M1 and nucleoprotein (NP) of IAV were shown to interact with actin filaments [6,7]. Recent reports have described the association of vRNP with microtubules and incorporation of α- and β-tubulin, the heterodimers of microtubules into IAV particles [8–10]. Further, we recently have shown the cleavage of tubulin deacetylase histone deacetylase 6 (HDAC6) by IAV-induced caspase-3 in infected cells [11]. Microtubules-based transport machinery helps many viruses to effect their movement within the cell [2]. Our hypothesis is that IAV modulates the microtubule cytoskeleton to facilitate the transport of viral components. Therefore, we are investigating the modulation of microtubule network and its significance during IAV replication. Here, we show that IAV induces the acetylation of α-tubulin in epithelial cells.

2. Materials and methods

2.1. Cells, virus, and plasmids

Madin-Darby canine kidney (MDCK) and normal human bronchial epithelial (NHBE) (provided by Greg Conner, University of Miami) cells were grown in MEM (Invitrogen) and BEGM (Lonza), respectively. IAV (H1N1) New Caledonia strain was propagated in embryonated chicken eggs and titrated on MDCK cells. Plasmid pcDNA3 (Invitrogen) expressing human HDAC6 was provided by Tso-Pang Yao (Duke University). HDAC6 (D1088E) mutant has been described elsewhere [11].

Abbreviations: AcMTs, acetylated microtubules; AcTub, acetylated α-tubulin; BIM, bisindolylmaleimide; CdTB, *Clostridium difficile* toxin B; HDAC6, histone deacetylase 6; hpi, hour post-infection; IAV, influenza A virus; INF, infected; M1, matrix protein; mDia, mammalian diaphanous protein; MDCK, Madin-Darby canine kidney; MOI, multiplicity of infection; NHBE, normal human bronchial epithelial; Noc, nocodazole; NP, nucleoprotein; PBS, phosphate-buffered saline; TSA, trichostatin A; UNI, uninfected; vRNP, viral ribonucleoprotein

* Corresponding author. Address: 2425 Ridgecrest Drive, SE, Albuquerque, NM 87108, USA. Fax: +1 505 3488567.

E-mail address: mhusain@lrri.org (M. Husain).

0014-5793/$36.00 © 2010 Federation of European Biochemical Societies. Published by Elsevier B.V. All rights reserved.
doi:10.1016/j.febslet.2010.11.023

2.2. Infection and transfection

Cells were washed twice with phosphate-buffered saline (PBS). Virus inoculum, diluted in PBS and supplemented with 3 μg/ml trypsin was added to cells. After 1 h incubation at 37 °C, inoculum was removed and cells were washed once with PBS. Fresh MEM was added and cells were incubated at 37 °C for 24 h. In some experiments, MEM supplemented with bisindolylmaleimide (BIM), *Clostridium difficile* toxin B (CdTB), nocodazole (Noc) (Calbiochem) or trichostatin A (TSA) (Sigma-Aldrich) was added to cells after removing the inoculum and cells were incubated as above. To inactivate IAV, inoculum was exposed to 1–2 mJ of UV radiation. For transfection, 2–3 μg plasmid DNA and 4–5 μl Lipofectamine 2000 (Invitrogen) were diluted separately in OptiMEM I (Invitrogen), mixed and incubated for 20–30 min at room temperature. DNA-Lipofectamine complex was added to cells and cells were incubated for 24 h at 37 °C.

2.3. Western blotting

Cells were harvested, washed with PBS, and lysed in lysis buffer (50 mM Tris, pH 7.5, 150 mM NaCl, 1% Triton X-100, 0.5% SDS, and protease-inhibitor cocktail [Roche]). The whole cell lysate was resolved on 10% Bis–Tris or 7% Tris-acetate gels (Invitrogen) and proteins were transferred to nitrocellulose membrane. Membrane was probed with mouse anti-acetylated α-tubulin (anti-AcTub), anti-α-tubulin (Sigma-Aldrich), anti-NP (Chemicon), anti-RhoA (Cytoskeleton Inc.) or rabbit anti-actin (Abcam), anti-HDAC6 (Santa Cruz) primary antibodies followed by HRP-conjugated donkey anti-mouse (Affinity BioReagents) or anti-rabbit (Pierce) secondary antibodies, respectively. Protein bands were developed with chemiluminescent kit (Thermo). All the Western blotting steps were performed at room temperature. To re-probe the same membrane with another antibody, membrane was stripped with Restore buffer (Thermo) for 20–30 min at 37 °C.

2.4. siRNA-mediated knockdown

Pre-designed target specific siRNA oligonucleotides against HDAC6 (Catalogue No. sc-35544) and RhoA (Catalogue No. sc-29471) genes were purchased from Santa Cruz Biotech. Oligonucleotides (50 nM) were transfected into cells using 2 μl Lipofectamine RNAiMax (Invitrogen) as described above. After 24–48 h incubation at 37 °C, cells were infected and analyzed by Western blotting as above.

2.5. Real time RT-PCR

Cells were grown on transwell filters (Corning) and infected from apical side. At 24 h post-infection (hpi), apical media was collected and centrifuged at 2000×*g* for 5 min. Viral RNA was then isolated from the media by using QIAamp kit (Qiagen). A quantitative real time RT-PCR assay was performed using viral RNA as a template to amplify IAV M1 gene, in vitro transcribed M1 RNA was used as standard. QuantiTect RT mix (Qiagen), RNA template, M1 forward primer (AGATTGCCGACTCCCAGCATAAGT), reverse primer (TGTTCACTCGATCCAGCCATTTGC), and probe (56-FAM/AGAAC AGAATGGTTCTGGCCAGCACT/3BHQ) were mixed and RT-PCR reaction was run on ABI 7900 thermocycler.

2.6. Virions preparation

Cells were grown on transwell filters and infected from apical side. At 24 hpi, apical media was collected, cleared off cell debris, and layered on 30% sucrose-NTE (100 mM NaCl, 10 mM Tris, pH 7.4, 1 mM EDTA) cushion and centrifuged at 250 000×*g* for 2 h at 4 °C in Beckman TLA55 rotor. The pellet was resuspended in sample buffer and analyzed by Western blotting.

3. Results

3.1. IAV-infected epithelial cells contain elevated levels of AcTub and α-tubulin

We recently demonstrated the cleavage of HDAC6 by IAV-induced caspase-3 in infected cells [11]. This indicated the potential regulation of HDAC6 activity in IAV-infected cells. Because HDAC6 is α-tubulin deacetylase [12], we investigated the acetylation of α-tubulin in IAV-infected cells. MDCK cells were infected with IAV, and total cell lysates were analyzed by Western blotting. We discovered that IAV-infected cells contained elevated level of AcTub (Fig. 1a). Over 2.5-times more AcTub was detected in infected cell lysate as compared to uninfected cell lysate (Fig. 1c). Interestingly, elevated levels of total α-tubulin (Fig. 1a) and β-tubulin (not shown) were also observed at the same time. Over 1.5-fold increase in total α-tubulin level was observed in infected cells (Fig. 1c), suggesting that IAV is potentially regulating the level of total tubulin too. To confirm these observations, levels of AcTub and total α-tubulin were analyzed in cells infected with IAV in the presence of BIM, an inhibitor of IAV replication [13] or with UV-inactivated IAV. No increase was observed in the level of either tubulin in BIM-treated infected cells (Fig. 1a) as well as cells infected with UV-inactivated IAV (Fig. 1b), suggesting that a productive IAV infection is required. Primary NHBE cells, which are the actual target of IAV in vivo, were used to further confirm the observations made in MDCK cells. Likewise, NHBE cells also showed elevated levels of acetylated and total α-tubulin after IAV infection (data not shown).

3.2. Activity of tubulin deacetylase HDAC6 is potentially downregulated in IAV-infected cells

To understand the mechanism of enhanced α-tubulin acetylation, cells were treated with TSA, an HDAC6 inhibitor [12]. As expected, after TSA treatment uninfected cells showed an increase in α-tubulin acetylation due to inhibition of HDAC6's deacetylase activity; however, TSA-induced increase in the acetylation of

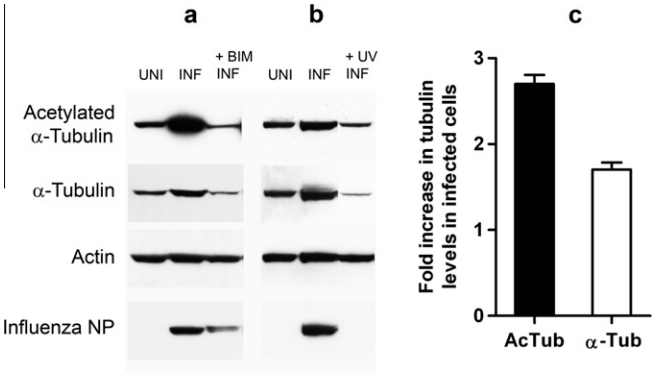

Fig. 1. IAV-infected cells contain elevated levels of AcTub and total α-tubulin. MDCK cells were infected with IAV at MOI of 0.5. Cells were treated with 20 μM BIM (a) or infected with UV-inactivated IAV (b) where indicated. At 24 hpi cells were lysed and total cell lysates were resolved on SDS–PAGE, and indicated proteins were detected by Western blotting. (c) Quantitation of increase in the amount of AcTub and α-tubulin in infected cells. The intensity of AcTub, α-tubulin, and actin bands was quantitated using Quantity One 4.0 software (Bio-Rad). The amount of AcTub and α-tubulin was normalized with actin amount, and was considered a 1-fold increase in uninfected (UNI) cells for comparisons to infected (INF) cells. Each bar represents the mean ± standard deviation (S.D.) for three independent experiments.

α-tubulin was significantly higher in infected cells (data not shown). This indicated that HDAC6 activity is potentially downregulated in infected cells, consequently resulting into elevated level of AcTub. To confirm this, expression of HDAC6 was knocked down by siRNA before IAV infection. Like TSA treatment, uninfected cells with reduced level of HDAC6 expression showed an increase in the acetylation of α-tubulin (Fig. 2b). Similarly, acetylation of α-tubulin was even higher in infected cells with knocked down expression of HDAC6 (Fig. 2b). To conversely confirm the downregulation of HDAC6 activity in IAV-infected cells, deacetylation efficiency of plasmid-expressed HDAC6 was compared in uninfected and infected cells. Plasmid-expressed HDAC6 was significantly effective in deacetylating the AcTub in uninfected cells (Fig. 2c), however, in infected cells, plasmid-expressed HDAC6 was moderately effective in deacetylating the AcTub (Fig. 2d). Over 57% AcTub was deacetylated by plasmid-expressed HDAC6 in uninfected cells as compared to only 34% in IAV-infected cells (Fig. 2e). This data further indicated that HDAC6 activity is downregulated in IAV-infected cells. To assess whether caspase-mediated cleavage of HDAC6 [11] is responsible for this, deacetylation of AcTub was analyzed in infected cells overexpressing the cleavage-resistant HDAC6 (D1088E) mutant. Like cleavage-sensitive wild type HDAC6, cleavage-resistant HDAC6 (D1088E) mutant also deacetylated the AcTub to a similar degree (Fig. 2d), suggesting that cleavage of HDAC6 by caspase-3 does not contribute to downregulation of its activity.

3.3. Rho GTPase is potentially involved in the downregulation of HDAC6 activity in IAV-infected cells

It has been demonstrated earlier that Rho GTPase regulates deacetylation of α-tubulin via HDAC6 [14]. To assess Rho GTPase's role in the enhanced acetylation of α-tubulin in IAV-infected cells, expression of Rho was knocked down by siRNA before infecting the cells with IAV. Consistent with Rho-mediated regulation of HDAC6 activity, uninfected cells with depleted Rho expression showed an increase in the acetylation of α-tubulin (Fig. 3b). Similarly, acetylation of α-tubulin was even higher in infected cells with knocked down expression of Rho (Fig. 3b), indicating a Rho-mediated downregulation of HDAC6 activity in IAV-infected cells. Almost identical results were obtained when infected cells were treated with CdTB, an inhibitor of Rho activity (data not shown). To conversely confirm the involvement of Rho, infected cells were treated with Noc, a microtubule depolymerizing drug, which also activates the Rho activity [15]. We argued that if Rho is involved in the enhanced acetylation of α-tubulin then Noc treatment should result in the significant deacetylation of α-tubulin due to activation of Rho and subsequent activation of HDAC6. Indeed, Noc greatly diminished α-tubulin acetylation in uninfected cells (not shown). Similarly, we could not detect the AcTub in Noc-treated infected cells (Fig. 3c). Further, Noc significantly reduced the TSA-induced acetylation of α-tubulin in infected cells (Fig. 3d). Collectively, these data suggest that a Rho-mediated pathway is involved in the enhanced acetylation of α-tubulin in IAV-infected cells.

3.4. Acetylation of microtubules affects the release of IAV from infected cells

We next investigated the significance of enhanced α-tubulin acetylation during IAV replication. A time-course experiment revealed that increase in the levels of AcTub and α-tubulin occur simultaneously between 6 and 12 hpi and coincide with IAV growth phase (data not shown). These data indicated the potential role of acetylated microtubules (AcMTs) in IAV assembly. Because microtubules are actively involved in the transport of viral components [2], we anticipated the role of AcMTs in the transport of IAV components and evaluated the effect of microtubule acetylation on IAV release from infected cells. For this, cells grown on transwell

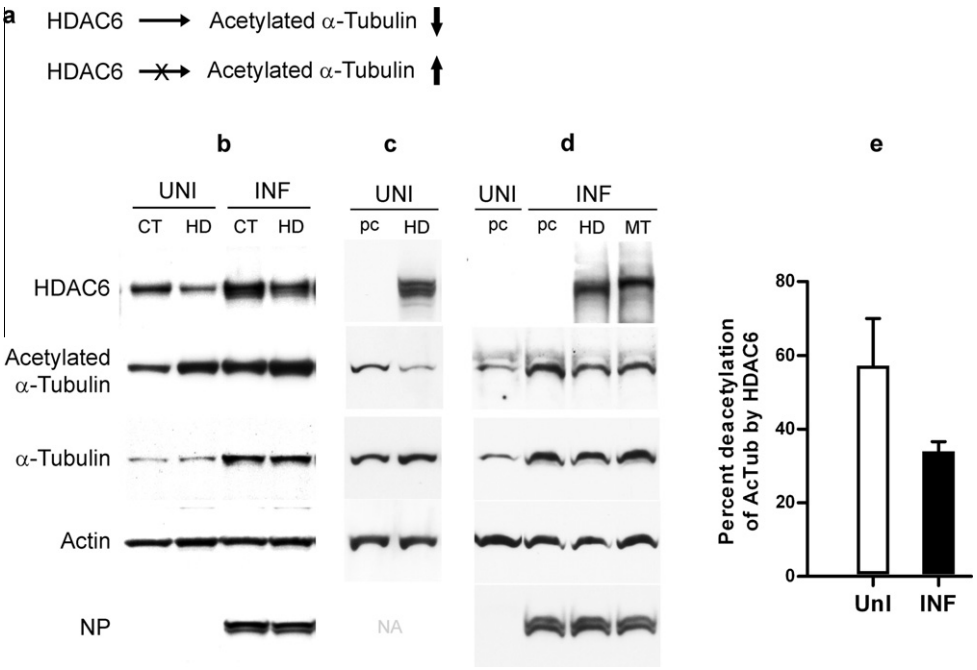

Fig. 2. (a) Schematic showing the effect of HDAC6 on AcTub. (b) siRNA-mediated knockdown of HDAC6 expression further increased the acetylation of α-tubulin in infected cells. NHBE cells were transfected with control (CT) or HDAC6 (HD) siRNAs for 24 h, and then infected and analyzed as Fig. 1. (c and d) Plasmid-expressed HDAC6 significantly or moderately deacetylated the α-tubulin in uninfected (UNI) (c) or infected (INF) (d) cells, respectively. MDCK cells were transfected with empty plasmid pcDNA3 (pc) or expressing wild-type HDAC6 (HD) or HDAC6 (D1088E) mutant (MT). Cells then were infected and analyzed as Fig. 1. (e) Quantitation of deacetylation of AcTub by plasmid-expressed HDAC6. The amount of AcTub was quantitated and normalized with actin as in Fig. 1c. AcTub amount detected in pcDNA3-transfected cells was considered 100% for comparisons to HDAC6-transfected cells. Each bar represents the mean ± S.D. for three independent experiments. NA, not applicable.

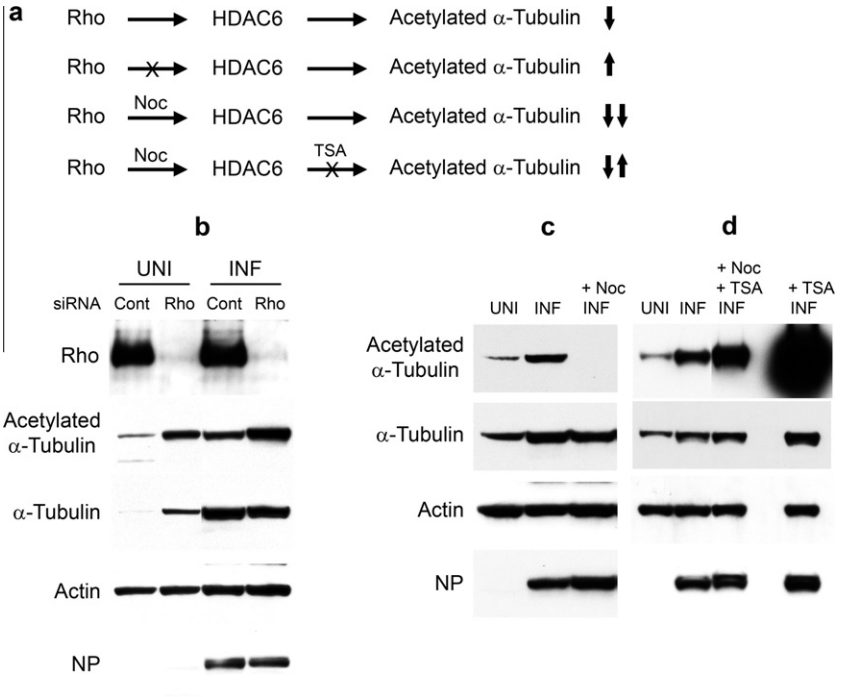

Fig. 3. (a) Schematic showing the effect of Rho on acetylation of α-tubulin. (b) siRNA-mediated knockdown of Rho expression further increased the acetylation of α-tubulin in infected cells. MDCK cells were transfected with control (Cont) or Rho siRNAs for 48 h, and then infected and analyzed as Fig. 1. (c and d) Noc induces the deacetylation of AcTub in infected cells. MDCK cells were infected and analyzed as Fig. 1. Noc (30 μM) and/or TSA (3 μM) were included in the medium where indicated. For presentation, some lanes are joined together from different parts of the same blot. UNI, uninfected; INF, infected.

filter supports were infected and treated with Noc or TSA. Viral RNA was isolated from the apical media collected from mock-treated, Noc-treated and TSA-treated infected cells and used as a template to amplify IAV M1 gene using real time RT-PCR. More than 3-fold reduction in M1 gene copies was detected in the apical media of Noc-treated infected cells as compared to mock infection (Fig. 4a). Conversely, over 3-fold increase in the M1 copy numbers was detected in the apical media of TSA-treated infected cells as compared to mock-treated cells (Fig. 4a). Almost identical results were obtained when virions were sedimented by ultracentrifugation from the apical media of mock-treated, Noc-treated and TSA-treated infected cells and detected by Western blotting using anti-NP antibody (Fig. 4b). These data suggest that AcMTs are potentially involved in the trafficking of IAV components.

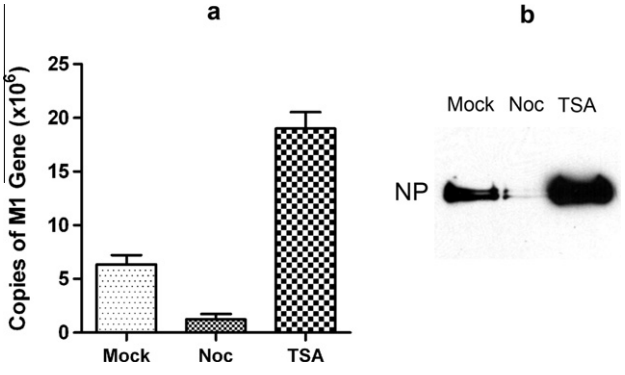

Fig. 4. Depolymerization/deacetylation and enhanced acetylation of microtubules decreased and increased, respectively, the release of IAV from infected cells. MDCK cells were grown on transwell filters and infected with IAV at MOI of 0.1. Noc (30 μM) or TSA (30 nM) was included in the medium where indicated. (a) Quantitative real time RT-PCR of M1 gene was performed using the viral RNA template isolated from apical media of mock-treated, Noc-treated or TSA-treated infected cells. Each bar represents the mean ± S.D. for three independent infections. (b) Released virions were isolated from apical media of mock-treated, Noc-treated or TSA-treated infected cells by ultracentrifugation. Virions were resuspended directly in sample loading buffer, resolved on SDS–PAGE, and detected by Western blotting.

4. Discussion

We have shown here the upregulation of acetylation of α-tubulin after IAV infection in non-polarized as well as polarized (not shown) epithelial cells. Further, enhancement in the level of total α-tubulin also was observed in IAV-infected cells. Because of the potential involvement of AcMTs in the trafficking of IAV components we initially focused on understanding the mechanism of enhanced acetylation of α-tubulin. At this point, we do not know the mechanism of elevated level of total tubulin in infected cells and currently working on it. Increase in total tubulin level may not be due to increased tubulin synthesis because IAV, mostly through its NS1 protein has been shown to shut off host protein synthesis [16]. In contrast, NS1 also has been shown to enhance the protein translation [17]. Therefore, it is likely that IAV differentially regulates the protein synthesis in infected cells though this needs to be examined with respect to tubulin. Alternatively, IAV could be regulating the stability of tubulin polypeptides in infected cells.

The siRNA-mediated knockdown and overexpression of HDAC6 suggested that HDAC6 activity was potentially downregulated in infected cells, consequently resulting into elevated level of AcTub. In addition, IAV may also be regulating the activity of α-tubulin acetylase to enhance the level of AcTub. Because, there also was a simultaneous increase in the level of total α-tubulin after IAV infection it is possible that newly appeared α-tubulin was greatly acetylated. In the future we may be able to test this event because, at present, mechanism of α-tubulin acetylation is not understood. The caspase-3-mediated cleavage of HDAC6 did not contribute to

downregulation of HDAC6 activity as both cleavage-sensitive and cleavage-resistant HDAC6s deacetylated the α-tubulin in infected cells to similar extents when overexpressed. On the other hand, a Rho-mediated regulation of HDAC6 activity was evident in IAV-infected cells. Rho family GTPases, which include Rho, Rac, and Cdc42, are activated from inactive GDP-bound to active GTP-bound state in response to stimuli. The activated Rho GTPases act on downstream effectors like p21-activated protein kinase, Rho-associated coiled-coil-containing protein kinase, neuronal Wiskott-Aldrich syndrome protein, mammalian diaphanous protein (mDia) and regulate the organization of cytoskeletal elements. The additional enhancement of α-tubulin acetylation due to silencing of Rho gene and abolition of acetylation in the presence of Rho activator Noc clearly suggest that Rho is potentially modulating the HDAC6 activity in IAV-infected cells. At this point, however, we do not know which Rho effector is involved in the downstream signaling and regulation of HDAC6 activity in IAV-infected cells. A Rho-mDia-HDAC6 pathway has been shown to regulate the microtubule acetylation in osteoclasts [14]. Future investigations will reveal the signaling mechanisms upstream and downstream of Rho in IAV-infected cells. In addition, Rho also could be involved in increased level of total α-tubulin because when expression of Rho was repressed in uninfected cells the amount of α-tubulin considerably went up (Fig. 3b); however, this observation needs further investigations. On the other hand, repression (Fig. 2b) or overexpression (Fig. 2c and d) of HDAC6 did not alter the level of total α-tubulin in either uninfected or infected cells as compared to the respective controls.

For IAV assembly all viral components must be transported to apical surface of plasma membrane. However, little is known about the involvement of cellular pathways and mechanism of the transport of vRNP and M1 to assembly site. Recent reports have demonstrated the association of vRNP with the microtubules [8,9] suggesting a role for microtubules in the transport of vRNPs, however, a potential mechanism remains to be elucidated. Acetylation is one of the post-translational modifications of α-tubulin [18]; therefore, IAV is modulating the post-translational modifications of microtubules in infected cells. This is a novel finding, which could have implications in understanding the polarized transport of IAV components to apical plasma membrane. Post-translational modifications tend to stabilize the microtubules, which then preferentially promote the polarized protein trafficking [18]. Recently, some viruses have been shown to modulate the acetylation of microtubules to facilitate delivery of virions to subcellular replication sites [19–21]. We have demonstrated here the enhanced acetylation of microtubules in IAV-infected cells, and decrease in the release of virions due to microtubule depolymerization/deacetylation and an increase due to enhanced microtubule acetylation. However, decrease in virions released after Noc treatment was not significantly higher. This suggests that without AcMTs, IAV components would randomly diffuse in the cytoplasm of infected cells and reach the plasma membrane in a non-polarized fashion, likely resulting in reduced or inefficient virion assembly and release. Future studies will elucidate the role of AcMTs in the polarized trafficking of IAV components.

Acknowledgments

We thank Jesse vanWestrienen, Richard Jaramillo, and Dr. Jennifer Tipper for technical assistance.

References

[1] Radtke, K., Döhner, K. and Sodeik, B. (2006) Viral interactions with the cytoskeleton: a hitchhiker's guide to the cell. Cell. Microbiol. 8, 387–400.
[2] Leopold, P.L. and Pfister, K.K. (2006) Viral strategies for intracellular trafficking: motors and microtubules. Traffic 7, 516–523.
[3] Nayak, D.P., Balogun, R.A., Yamada, H., Zhou, Z.S. and Barman, S. (2009) Influenza virus morphogenesis and budding. Virus Res. 143, 147–161.
[4] Cheung, T.K.W. and Poon, L.L.M. (2007) Biology of influenza A virus. Ann. N. Y. Acad. Sci. 1102, 1–25.
[5] Schmitt, A.P. and Lamb, R.A. (2005) Influenza virus assembly and budding at the viral budozone. Adv. Virus Res. 64, 383–416.
[6] Avalos, R.T., Yu, Z. and Nayak, D.P. (1997) Association of influenza virus NP and M1 protein with cellular cytoskeletal elements in influenza virus infected cells. J. Virol. 71, 2947–2958.
[7] Husain, M. and Gupta, C.M. (1997) Interactions of viral matrix protein and nucleoprotein with the host cell cytoskeletal actin in influenza viral infection. Curr. Sci. 73, 40–47.
[8] Mayer, D., Molawi, K., Martinez-Sobrido, L., Ghanem, A., Thomas, S., Baginsky, S., Grossmann, J., García-Sastre, A. and Schwemmle, M. (2007) Identification of cellular interaction partners of the influenza virus ribonucleoprotein complex and polymerase complex using proteomic-based approaches. J. Proteome Res. 6, 672–682.
[9] Momose, F., Kikuchi, Y., Komase, K. and Morikawa, Y. (2007) Visualization of microtubule-mediated transport of influenza viral progeny ribonucleoprotein. Microb. Infect. 9, 1422–1433.
[10] Shaw, M.L., Stone, K.L., Colangelo, C.M., Gulcicek, E.E. and Palese, P. (2008) Cellular proteins in influenza virus particles. PLoS Pathog. 4, e1000085.
[11] Husain, M. and Harrod, K.S. (2009) Influenza A virus-induced caspase-3 cleaves the histone deacetylase 6 in infected epithelial cells. FEBS Lett. 583, 2517–2520.
[12] Hubbert, C., Guardiola, A., Shao, R., Kawaguchi, Y., Ito, A., Nixon, A., Yoshida, M., Wang, X.F. and Yao, T.P. (2002) HDAC6 is a microtubule-associated deacetylase. Nature 417, 455–458.
[13] Root, C.N., Wills, E.G., McNair, L.L. and Whittaker, G.R. (2000) Entry of influenza virus into cells is inhibited by a highly specific protein kinase C inhibitor. J. Gen. Virol. 81, 2697–2705.
[14] Destaing, O., Saltel, F., Gilquin, B., Chabadel, A., Khochbin, S., Ory, S. and Jurdic, P. (2005) A novel Rho-mDia2-HDAC6 pathway controls podosome patterning through microtubule acetylation in osteoclasts. J. Cell Sci. 118, 2901–2911.
[15] Chang, Y.C., Nalbant, P., Birkenfeld, J., Chang, Z.F. and Bokoch, G.M. (2008) GEF-H1 couples nocodazole-induced microtubule disassembly to cell contractility via RhoA. Mol. Biol. Cell 19, 2147–2153.
[16] Chen, Z. and Krug, R.M. (2000) Selective nuclear export of viral mRNAs in influenza-virus-infected cells. Trends Microbiol. 8, 376–383.
[17] Salvatore, M., Basler, C.F., Parisien, J.P., Horvath, C.M., Bourmakina, S., Zheng, H., Muster, T., Palese, P. and Garcia-Sastre, A. (2002) Effects of influenza A virus NS1 protein on protein expression: the NS1 protein enhances translation and is not required for shutoff of host protein synthesis. J. Virol. 76, 1206–1212.
[18] Hammond, J.W., Cai, D. and Verhey, K.J. (2008) Tubulin modifications and their cellular functions. Curr. Opin. Cell Biol. 20, 71–76.
[19] Naranatt, P.P., Krishnan, H.H., Smith, M.S. and Chandran, B. (2005) Kaposi's sarcoma-associated herpesvirus modulates microtubule dynamics via RhoA-GTP-diaphanous 2 signaling and utilizes the dynein motors to deliver its DNA to the nucleus. J. Virol. 79, 1191–1206.
[20] Valenzuela-Fernandez, A., Álvarez, A.S., Gordon-Alonso, M., Barrero, M., Ursa, A., Cabrero, J.R., Fernandez, G., Naranjo-Suarez, S., Yanez-Mo, M., Serrador, J.M., Munoz-Fernandez, M.A. and Sanchez-Madrid, F. (2005) Histone deacetylase 6 regulates human immunodeficiency virus type 1 infection. Mol. Biol. Cell 16, 5445–5454.
[21] Warren, J.C., Rutkowski, A. and Cassimeris, L. (2006) Infection and replication-deficient adenovirus induces changes in the dynamic instability of host cell microtubules. Mol. Cell. Biol. 17, 3557–3568.